Available online at www.sciencedirect.com
SCIENCE DIRECT
Biochimica et Biophysica Acta 1744 (2005) 199–212
BIOCHIMICA ET BIOPHYSICA ACTA
BBA
http://www.elsevier.com/locate/bba

NADPH oxidase homologs are required for normal cell differentiation and morphogenesis in *Dictyostelium discoideum*

Bernard Lardy[a,b,*], Mireille Bof[a], Laurence Aubry[a], Marie Hélène Paclet[b], Françoise Morel[b], Michel Satre[a], Gérard Klein[a]

[a]*Laboratoire de Biochimie et Biophysique des Systèmes Intégrés (UMR5092 CNRS), Département de Réponse et Dynamique Cellulaires, CEA-Grenoble, 38054 Grenoble Cedex 9, France*
[b]*Groupe de Recherche et d'Etude du Phénomène Inflammatoire (GREPI)-(EA 2938), Laboratoire d'Enzymologie, Centre Hospitalier Universitaire de Grenoble, BP 217, 38043 Grenoble, France*

Received 14 December 2004; received in revised form 25 January 2005; accepted 4 February 2005
Available online 8 March 2005

Abstract

Membrane-associated NADPH oxidase complexes catalyse the production of the superoxide anion radical from oxygen and NADPH. In mammalian systems, NADPH oxidases form a family of at least seven isoforms that participate in host defence and signalling pathways. We report here the cloning and the characterisation of slime mould *Dictyostelium discoideum* homologs of the mammalian heme-containing subunit of flavocytochrome *b* (gp91^{phox}) (NoxA, NoxB and NoxC), of the small subunit of flavocytochrome *b* (p22^{phox}) and of the cytosolic factor p67^{phox}. Null-mutants of either *noxA*, *noxB*, *noxC* or *p22^{phox}* show aberrant starvation-induced development and are unable to produce spores. The overexpression of NoxA$_{myc2}$ in *noxA* null strain restores spore formation. Remarkably, the gene *alg-2B*, coding for one of the two penta EF-hand proteins in *Dictyostelium*, acts as a suppressor in *noxA*, *noxB*, and *p22^{phox}* null-mutant strains. Knockout of *alg-2B* allows *noxA*, *noxB* or *p22^{phox}* null-mutants to return to normal development. However, the knockout of gene encoding NoxC, which contains two penta EF-hands, is not rescued by the invalidation of *alg-2B*. These data are consistent with a hypothesis connecting superoxide and calcium signalling during *Dictyostelium* development.

Keywords: NADPH oxidase; *Dictyostelium*; Cell-type differentiation; EF-hand

1. Introduction

In mammalian neutrophils and other professional phagocytes, the NADPH oxidase (cytochrome *b*558) catalyses the production of the superoxide anion radical from oxygen and NADPH [1]. Chronic granulomatous disease (CGD) is characterised by the absence of NADPH oxidase activity [2]. Cytochrome *b*558 is a 1:1 heterodimer comprising two subunits, the catalytic core gp91^{phox} and p22^{phox} [3]. The enzyme is dormant in resting cells and its activation from the resting state results from the assembly of cytosolic regulatory proteins p47^{phox}, p67^{phox} and Rac1/2 with the membrane associated cytochrome *b*558, upon cell stimulation by pathogens or receptor-mediated stimuli (for reviews, [4–6]). Other protein components are also known to be associated with the NADPH oxidase, such as p40^{phox} [7,8] and the EF-hand containing calciproteins S100A8/A9, also known as MRP8/MRP14 [9,10]. In vitro, oxidase activity can be elicited by incubating membrane cytochrome *b*558 and cytosolic components in the presence of anionic amphiphiles [11].

The Nox family (for NADPH oxidase) has been broadened recently with the discovery of new isoforms [12]. Seven homologs of the neutrophil gp91^{phox} have been described up to now in non-phagocytic mammalian cells, all showing the four histidine ligands for two heme groups embedded within the membrane and the conserved regions

* Corresponding author. GREPI EA 2938, DBPC/Enzymologie, Hôpital Albert Michallon, BP 217-CHU Grenoble Cedex 9, France. Tel.: +33 476 76 54 83; fax: +33 476 76 56 08.
E-mail address: BLardy@chu-grenoble.fr (B. Lardy).

0167-4889/$ - see front matter © 2005 Elsevier B.V. All rights reserved.
doi:10.1016/j.bbamcr.2005.02.004

characteristic of NADPH and FAD binding sites (for reviews, see [13–15]). Among these homologs, Nox1, Nox3 and Nox4 have a size similar to that of gp91^{phox} (Nox2), while the others have N-terminal extensions, containing four Ca^{2+}-binding EF-hands for Nox5 [16], and two EF-hands and a large peroxidase domain for both Duox1 and Duox2 [17]. Duox1 and Duox2 are involved in the H_2O_2 production associated with thyroperoxidase in the thyroid [17,18]. Similarly to Nox2 in myeloid cells, Nox5 generates large amounts of superoxide in response to a cytosolic Ca^{2+} increase [19]. Some Nox isoforms are aberrantly expressed in several human cancers, with Nox4 being the isoform most frequently reported. Nox1 displays a very low superoxide-producing activity, unless activated by two cytosolic factor homologs of p67^{phox} (NOXA1) and p47^{phox} (NOXO1) [16,19–21]. The overexpression of Nox1 is associated to tumorigenesis, in particular through the activation of angiogenesis [22,23].

Plant cells exposed to pathogens produce an oxidative burst, and genes coding for respiratory burst oxidase homologs (*rboh*) have been characterised in *Arabidopsis thaliana* and in other plants [24]. These all show an N-terminal extension, with one or two EF-hand motifs [25,26]. Accordingly, superoxide production is stimulated by Ca^{2+} [27]. Apart from their involvement in the defence response, plant NADPH oxidases participate in cell death signalling [26] and in Ca^{2+}-dependent root elongation [24].

It has been suggested that the appearance of Nox genes accompanies the emergence of multicellular structures providing signalling systems that ensure harmonious development [28]. *Dictyostelium discoideum* is an appropriate biological organism to test this hypothesis, as this social amoeba is at the boundary between unicellular and multicellular life [29]. In addition, *D. discoideum* is a professional phagocyte in its vegetative stage, feeding efficiently on bacterial preys [30–32]. Whether or not a functional NADPH oxidase is needed for this process is an additional question that triggered our interest.

In this work, we have identified NADPH oxidase components in *D. discoideum*, including three flavocytochrome *b*558 large subunit isoforms (NoxA, NoxB, and NoxC) with the six transmembrane pillars and the four histidines coordinating the two hemes characteristic of mammalian gp91^{phox} (Nox2). NoxC shows an N-terminal extension, with two EF-hand motifs. Furthermore, we have characterised amoebal homologs of p22^{phox}, the flavocytochrome *b*558 small subunit, and of p67^{phox}, an essential cytosolic activation factor in mammals. The inactivation of the genes coding for *Dictyostelium* p22^{phox}, NoxA, NoxB, and NoxC leads to developmental defects. We also report the rescue of the noxA, noxB and p22^{phox} knockout by the disruption of the penta EF-hand protein ALG-2 (Apoptosis-linked gene-2) implying a potential cross-talk between superoxide and Ca^{2+} signalling in *Dictyostelium* cell differentiation decisions.

2. Materials and methods

2.1. Cloning and sequencing D. discoideum noxA, -B, -C, $p22^{phox}$ and $p67^{phox}$ genes

Oligonucleotide primers were designed on the basis of relevant clones in the *Dictyostelium* genomic database (http://dictybase.org, [33]). Coding sequences were obtained by a combination of RT-PCR and 5′- and 3′-RACE experiments on whole RNA. The full-length genomic sequences were derived from PCR experiments on genomic DNA. The sequences for *Dictyostelium noxA*, *-B*, *-C*, $p22^{phox}$ and $p67^{phox}$ have been deposited at GenBank™ under accession numbers AF123275, AY221173, AY224390, AY221170/AY221171 and AY221172/AY224389, and they are now referenced in dictyBase (http://dictybase.org, [33]) as DDB0191274, DDB0191445, DDB0191391, DDB019134 and DDB0191152, respectively.

2.2. Generation of mutants and plasmid constructs

The single *noxA*, *-B*, *-C* and $p22^{phox}$ null mutants were produced in JH10 (a thymidine auxotrophic strain derived from KAx-3), by inserting the blasticidin S cassette *bsr* [34] at positions 1028 (*noxA*), 1518 (*noxB*), 964 (*noxC*) and 443 ($p22^{phox}$) of the genomic DNAs, respectively. To obtain the double knockout $noxA^-/noxB^-$, a *noxA*-deficient strain was first generated in the JH10 strain using the *thy1* selection cassette [35], and then invalidated in the *noxB* gene, using the *bsr* cassette as described above. For the double knockout mutants $alg\text{-}2B^-/noxA^-$, $alg\text{-}2B^-/noxB^-$, $alg\text{-}2B^-/noxC^-$ and $alg\text{-}2B^-/p22^{phox-}$, the *bsr* cassette insertions were done in an *alg-2B* null JH10 strain constructed using the *thy1* selection cassette as described previously [36]. Transformants were cloned by plating cells on SM-agar plates in the presence of *Klebsiella aerogenes.* The existence of potential gene knockout clones was confirmed by Southern blot.

The *alg-2B* and *noxA* overexpression constructs were produced in pEXP4$^+$ (neomycin resistance neo^r) using the *act15* promoter to control the expression of full-length ALG-2B or full-length NoxA protein tagged at the C-terminus with a double myc epitope ($NoxA_{myc2}$).

2.3. Cell culture and development

The JH10 strain was grown in an axenic medium containing 100 μg/ml thymidine. JH10-derived knockout strains were grown in suspension in a HL5 medium, without added thymidine when the *thy1* selection cassette was used and in the presence of 7.5 μg/ml blasticidin when the *bsr* selection cassette was used. The ALG-2B and $NoxA_{myc2}$ overexpressing strains were grown in a medium containing G418 (20 μg/ml). Growth curves for the various knockout mutants were determined in axenic medium or on *K. aerogenes* plates.

Development was monitored by plating cells on non-nutritive Na/K–Pi-buffered agar plates, after the removal of nutritive medium.

2.4. Gene expression during development

The expression of the various genes during development was assessed using RT-PCR on whole RNA isolated from vegetative amoebae and from cells that had been filter-developed on non-nutritive Na/K–Pi-buffered agar plates for 4, 8, 12, 16, 20 or 24 h, or spores and stalks [37]. One-step RT-PCR was performed using the QIAGEN kit as suggested by the manufacturer, and, whenever possible, using primers spanning intron/exon boundaries (Table 1). The number of PCR cycles was adjusted so as to obtain a non-saturating response.

2.5. Cell type separation

JH10 amoebae were allowed to develop on non-nutritive Na/K–Pi-buffered agar plates until mature fruiting bodies were obtained. Mature spores were harvested by shaving spore heads with a glass slide. Remaining stalks were then scraped from the plates and washed free of remaining spores on a fritted filter (40–100 μm porosity). Spores and stalks were washed in PBS buffer.

2.6. Expression of cell type specific genes

Cells carrying the *SP60/lacZ*, *SpiA/lacZ*, and *ecmA/lacZ* reporter constructs were left to develop on nitrocellulose filters laid on non-nutritive agar plates and subjected to β-galactosidase staining [38,39].

2.7. Activity measurements

In vitro reconstitution of an active oxidase complex was assayed in a cell-free assay [40,41]. Briefly, membranes (30 μg of protein) were mixed with the cytosol (300 μg of protein) in a medium for oxidase reconstitution containing 40 μM GTPγS, 5 mM $MgCl_2$, and a variable quantity (40–100 nmol) of anionic amphiphiles, either arachidonic acid or lithium dodecyl sulfate, in a final volume of 100 μl. After incubation for 10 min at 25 °C, the solution was transferred to a photometric cuvette filled with 100 μM cytochrome *c*, 150 μM NADPH, PBS buffer in a final volume of 900 μl. Superoxide production was determined as the superoxide dismutase-sensitive portion of cytochrome *c* reduction recorded at 550 nm (extinction coefficient 21,000 M^{-1} cm^{-1}). As an alternative, the reduction of tetrazolium dyes by whole cells was monitored using nitroblue tetrazolium (NBT) [23], or 2,3-bis(2-methoxy-4-nitro-5-sulfophenyl)-5-[(phenylamino)carbonyl]-2H-tetrazolium hydroxide (XTT). The XTT assay was conducted as described previously [42] using 10 mM Tiron to determine the degree of reduction which was due to the superoxide. The quantity of super-

Table 1
Primer sequences for RT-PCR analysis

mRNA	Forward primer	Reverse primer	Expected size (bp)
NoxA	5′-GCATTTGTTTACACATTTGTTCATTATTAT	5′-ATCCTCCTCGGGTGCTGATGT	786
NoxB	5′-TGTACAATTATTCATTGGGTTGGT	5′-TGGATGCCACTCATGGTATGC	550
NoxC	5′-GATAAAATTTTAATGGAGAGTTTAAAAGAAAATGAG	5′-CTCTACAGGGATTGGGAAAGA	457
$p22^{phox}$	5′-GATATATAGCAATCTATTCAATTTGTGTTG	5′-TCGTTGGTGAAGCGTTAGATA	389
$p67^{phox}$	5′-TCATATGAATTCAGAGTTAAATCATGC	5′-GTTTGGATCCAGATGAAGATTGAATTGAAGAAGATGTTGC	361
Casein kinase II	5′-GAACTATGAAGCTTTAAATGTTAAATGGGAAACTC	5′-TGGTTTAACATCTCTATGCATGATACCGTT	406

oxide produced was calculated using the molar extinction coefficient 21,600 M^{-1} cm^{-1} at 470 nm.

3. Results

3.1. Dictyostelium is endowed with three superoxide-generating NADPH oxidase flavocytochrome large subunit homologs, but a single NADPH oxidase small subunit homolog

The capacity of *Dictyostelium* to phagocytose bacteria prompted us to explore whether amoebae use NADPH oxidase homologs in this process. RACE-, genomic- and RT-PCR experiments allowed us to fully sequence the genes coding for three NADPH oxidase homologs, *noxA*, *noxB* and *noxC* genes. All three homologs contained the canonical features of Nox proteins and sequence alignments [43] showed that regions proposed as binding sequences for flavin and pyridine nucleotides are highly conserved between human Nox2 (gp91^{phox}), the NADPH-oxidase prototype, and *Dictyostelium* NoxA, -B and -C. The full length NoxA, and the NADPH-oxidase core of NoxB and NoxC, as defined in Fig. 1A, are 38% (66), 34% (67) and 25% (55) identical (homologous) to the Nox2 protein, respectively. The third and fifth predicted transmembrane segments, as proposed in the gp91^{phox} model [3], contained the conserved histidines that serve as ligands for the two hemes. All amino acids the mutation of which leads to CGD (X+) (R54, A57, H303, P304, H338, P415 and D500) are conserved in the three *Dictyostelium* Nox sequences (for review, [44]). In NoxC, a 560-residue N-terminal extension (Fig. 2A) is present that harbours two EF-hands (aa 466–494 and aa 510–538), a feature also found in plant NADPH oxidases [26]. NoxC EF-hands belong to the calcineurin B subgroup and their alignment with human Nox5 EF-hands [16] is shown in Fig. 2B. In the phylogenetic tree generated with the Nox amino acid sequences trimmed to the Nox2 core (Fig. 2C), *Dictyostelium* NoxC branched close to human Nox5, an indication that in addition to the presence of EF-hands in both proteins, the core sequences contain additional signal(s) of relatedness.

Three sites of interaction with p47^{phox} have been mapped on gp91^{phox} using peptide inhibition of the active oxidase assembly (S87 to L94, F451 to L458 and E555 to F564) [45]. *Dictyostelium* Nox isoforms lack two of the three sites of interaction with p47^{phox} and the remaining site corresponds to a peptide with a very low inhibitory potency [45], suggesting that amoebal Nox isoforms may not be able to interact with p47^{phox}.

The identification of three large subunits of the catalytic core of *Dictyostelium* NADPH oxidases encouraged us to search for the other components of the phagocyte flavocytochrome complex. We have cloned a gene coding for a *Dictyostelium* homolog of mammalian *p22^{phox}* and sequence alignment [43] with human p22^{phox} is shown in Fig. 1B. The observed overall identity (similarity) match is significant, as it comprises 41 identical and more than 40 similar residue pairs. Noteworthy features in *Dictyostelium* p22^{phox} are the absence of a central 18-amino acid stretch (human p22^{phox} aa 56–73) and of the C-terminal-proline-rich tail, two regions implicated in the binding of the cytosolic factor p47^{phox} [46,47].

3.2. Cytosolic factor complement in Dictyostelium is restricted to a p67^{phox} homolog

We have also cloned a homolog from *Dictyostelium* of the cytosolic factor p67^{phox} (Fig. 3A). Domain analysis showed the characteristic N-terminal 4-tetratricopeptide repeats (TPR1-4), a central PB1 region framed by several proline-rich motifs and a C-terminal WW domain (Fig. 3A–B). Taking into account the functional analogy between WW and SH3 domains [48], the overall *Dictyostelium* p67^{phox} domain arrangement is quite similar to that found in mammalian p67^{phox} and in the Nox activator 1 (NOXA1) [20,21,49]. This suggests a possible intramolecular interaction between the WW domain and an upstream PPSY sequence (Fig. 3B). Comparative protein modelling performed on the SWISS-MODEL server (http://swissmodel.expasy.org/), using the human p67^{phox} (aa 1–213) structure [50] as a template, showed a very satisfactory adjustment (Fig. 3C). Noteworthy in Fig. 3C is the high degree of conservation of the 20 amino acid hairpin insertion between TPR3 and TPR4, involved in the interface between Rac and p67^{phox} [51]. *Dictyostelium* Arg-101 and Asp-107 correspond to human Arg-102 and Asp-108, respectively, identified as playing key roles in p67^{phox} complex formation with Rac. Other residues contributing to the interface, such as Ser-36 and Asp-66 [51], are conserved as well. Conversely, all the residues of Rac involved in the interface with p67^{phox} [51] are present in *Dictyostelium* Rac1A, -1B or -1C, which are the members of Rac GTPase subfamily [52,53] showing the greatest homologies to neutrophil Rac2.

Fig. 1. Multiple amino acid sequence alignment of the *D. discoideum* Nox proteins with human Nox2, and the *D. discoideum* p22^{phox} homolog with human p22^{phox}. (A) *D. discoideum* NoxA, NoxB (aa 168–698), NoxC (aa 583–1142), and human Nox2 (gp91^{phox}) were aligned using CLUSTAL W 1.7 software [43]; Dd, *D. discoideum*; Hs, *Homo sapiens*. The position of the six putative transmembrane domains (TM1-6), and the sequences involved in the binding of the two cofactors FAD and NADPH, are boxed. Grey shading was used at positions where amino acids were found to be identical at least in three out of the four sequences. The four conserved histidines in TM3 and TM5 acting as ligands for the two hemes are highlighted on a black background. The three Nox2 sequences in the first intracellular loop linking TM2 and TM3 and in the C-terminal domain involved in p47^{phox} binding [45] are underlined. (B) *D. discoideum* (Dd-p22^{phox}) and human p22 (Hs-p22^{phox}) were aligned (see above). The predicted transmembrane domains (TM1-3) are boxed, identical amino acids are highlighted by grey shading and the polyproline domain by black shading. The two regions of human p22^{phox} involved in p47^{phox} binding are underlined. Dd, *D. discoideum*; Hs, *H. sapiens*.

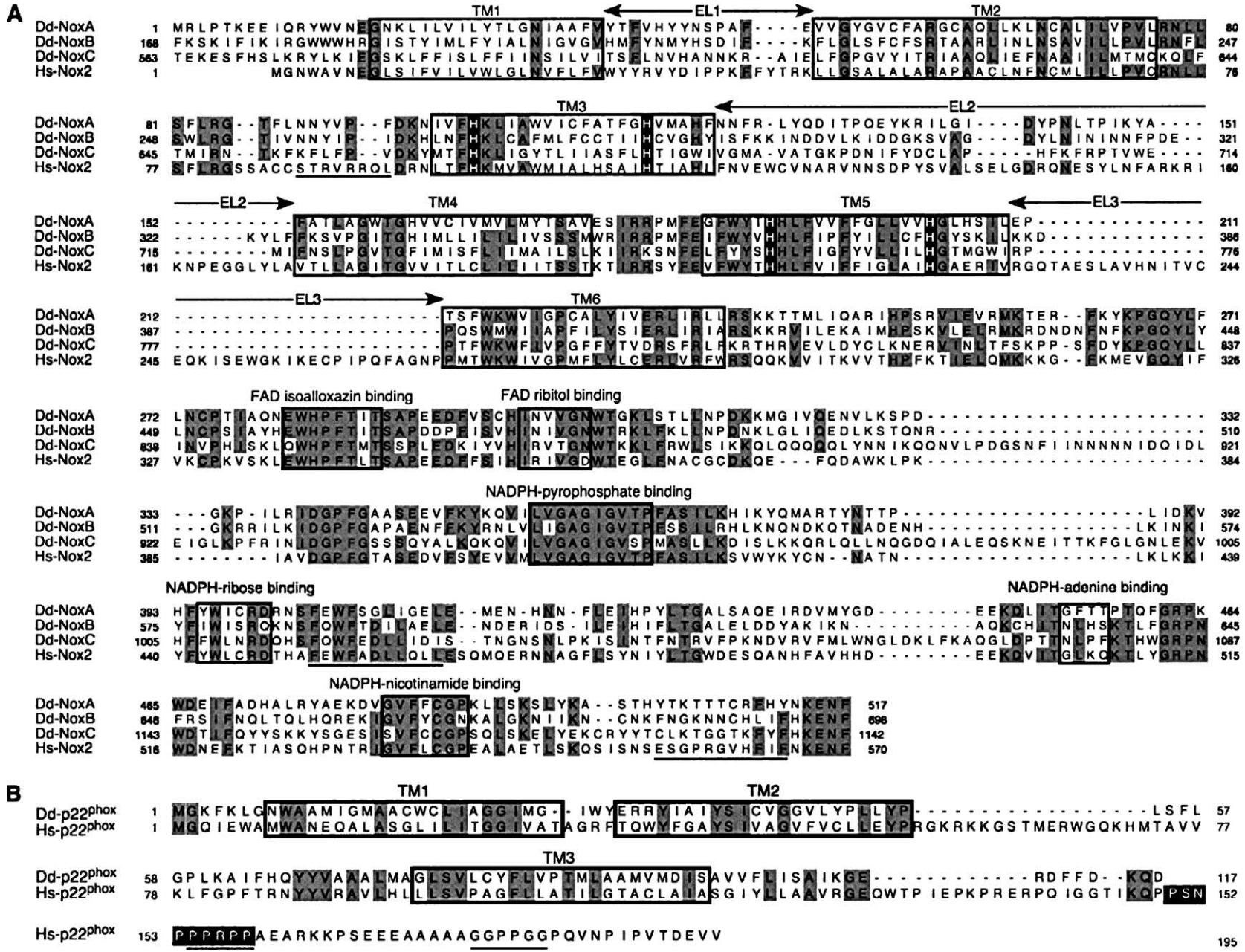
A
TM1
EL1
TM2
Dd-NoxA
Dd-NoxB
Dd-NoxC
Hs-Nox2
TM3
EL2
TM4
TM5
EL3
TM6
FAD isoalloxazin binding
FAD ribitol binding
NADPH-pyrophosphate binding
NADPH-ribose binding
NADPH-adenine binding
NADPH-nicotinamide binding
B
TM1
TM2
Dd-p22phox
Hs-p22phox
TM3
Hs-p22phox

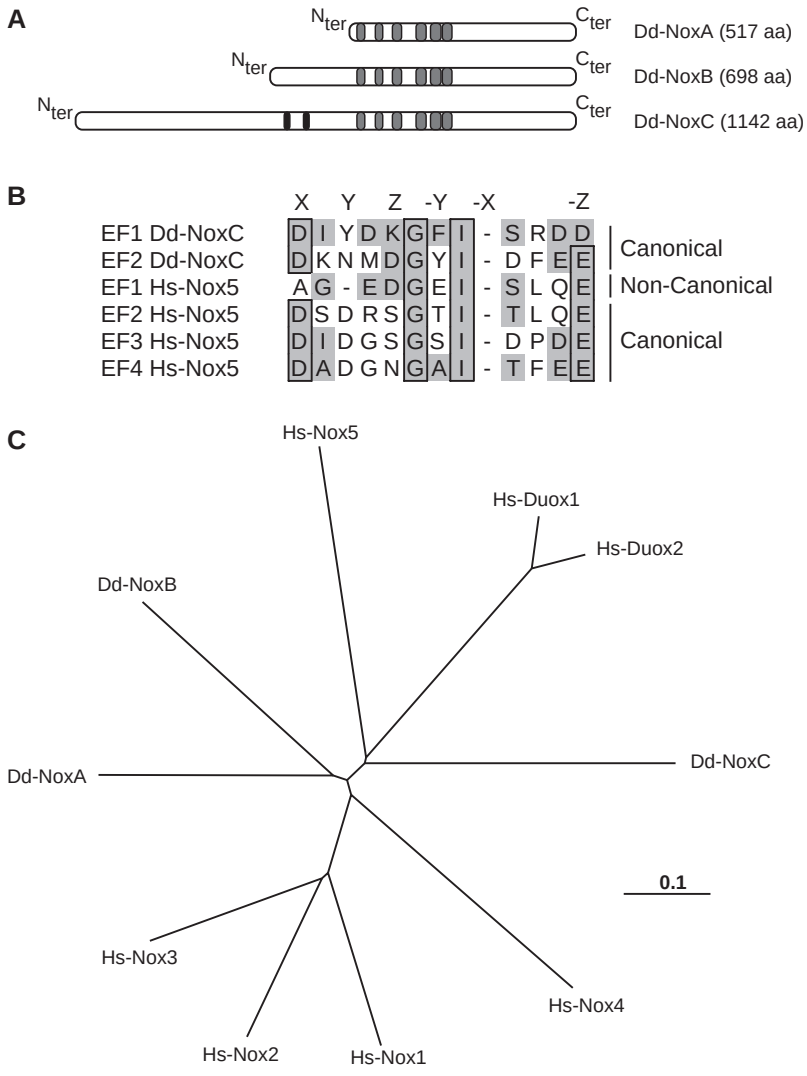

Fig. 2. Domain organisation and phylogenetic tree of Dd-Nox homologs. (A) Schematic organisation of *Dictyostelium* Nox proteins, showing the N-terminal extension in *Dictyostelium* NoxB and -C, the six predicted transmembrane domains (grey boxes) and the two EF-hands (Pfam 00036) in Dd-NoxC (black boxes). (B) Alignment of the EF-hand motifs from *Dictyostelium* NoxC and human Nox5; Dd, *D. discoideum*; Hs, *H. sapiens*. The residues that contribute to the pentagonal bipyramidal calcium co-ordination are labelled X, Y, Z, -Y, -X, and -Z. The water molecules that co-ordinate the calcium ion are indicated by a dash (position-X in all EF-hands and position Y in the non-canonical EF-hand). Identities between the proteins are boxed, and homologies are indicated on a grey background. (C) Phylogenetic relationship between Nox proteins. The Dd- and human Nox sequences were trimmed to the stretch common to all sequences (Nox2 length) and aligned [43]. The generated phylogenetic tree was visualised with NJ-plot software. GenBank™ accession numbers are the following: Nox1, AF127763; Nox2, NM-000397; Nox3, AF190122; Nox4, AF254621; Nox5, AF353089; Duox1, AF213465; and Duox2, AF267981. Dd, *D. discoideum*; Hs, *H. sapiens*.

The search in the *Dictyostelium* genome for other potential NADPH oxidase cytosolic components, namely $p47^{phox}$ and $p40^{phox}$, was unsuccessful.

3.3. NADPH-oxidase components display distinct developmental regulation and cell type specificity

In *Dictyostelium*, starvation initiates a developmental cycle. Starved amoebae chemotax towards cAMP secreted by surrounding starving cells. The formed aggregate develops into a migrating slug and fruiting body. The spores of the fruiting body are resistant to adverse conditions and eventually germinate into single amoebae under better conditions. To determine the steady state mRNA levels of the three *D. discoideum* NADPH oxidase genes, $p22^{phox}$ and $p67^{phox}$, RT-PCR analysis was performed with total RNA extracted from various developmental stages of the *D. discoideum* life cycle (Fig. 4A) and normalised to casein kinase II mRNA expression [54] (not shown, see Fig. 4B). The mRNA expression of *noxA* was found at a maximal level in vegetative amoebae, and decreased slightly (about 20%) during development. The level of *noxB* transcript increased during aggregation then showed a marked reduction in fruiting bodies. These data for *noxA* and *noxB* are in general agreement with the published results [55,56] showing a constant expression of

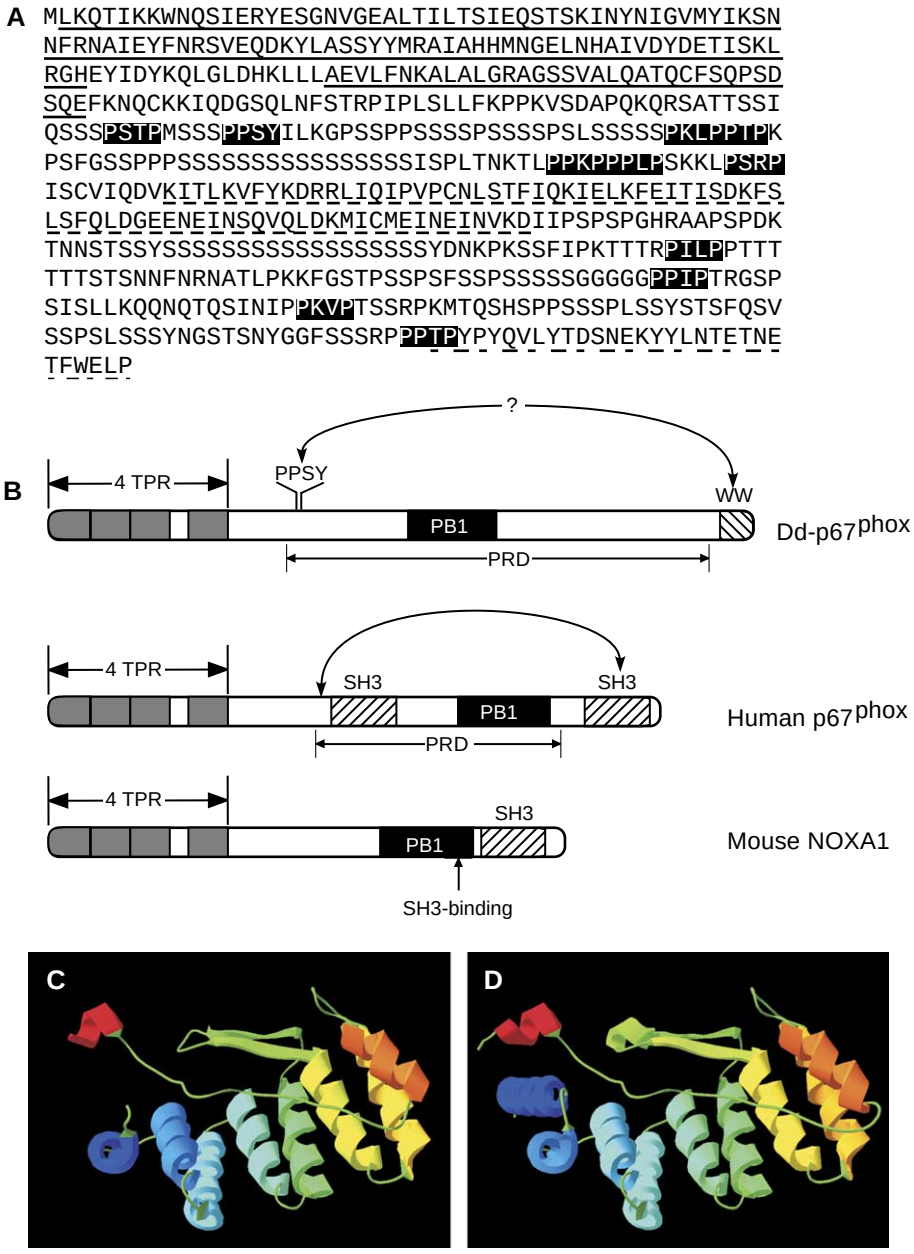

Fig. 3. Analysis of *D. discoideum* p67^{phox} homolog. (A) The four N-terminally localised TPR (tetratricopeptide repeat, Pfam 00515) units are underlined by a solid line and the central PB1 (Phox and Bem1, Pfam 00564) and the C-terminal WW domain (Pfam 00397) are underlined by dashed lines. Low complexity serine-rich stretches are localised on both sides of PB1. Several proline-rich motifs are highlighted in black. (B) Schematic domain arrangement of *Dictyostelium* p67^{phox} (Dd-p67^{phox}), human p67^{phox} (also known as NCF2 or NOXA2) and mouse NOXA1. In human p67^{phox}, the C-terminal SH3 domain interacts with the proline-rich domain (PRD) upstream of the first SH3 domain. An analogous intramolecular interaction is suggested in *Dictyostelium* p67^{phox}, through the possible binding of the C-terminal WW domain by an upstream WW-binding sequence (PPSY). (C) A homology structure of *Dictyostelium* p67^{phox} N-terminus was calculated by Swiss Model and visualised with Deep View Swiss-PDB using the structure of the 192 N-terminal residues of human p67^{phox} (1HH8) as a template [50]. The fit of helix A1 of the first TPR motif of *Dictyostelium* p67^{phox} to the corresponding element in human p67^{phox} was not accurate enough to be visualised. The structure was coloured according to secondary structure succession, with a transition from blue to red from the N-terminus to the end of the fragment. (D) The human p67^{phox} N-terminus structure (1HH8) is shown for comparison [50].

NoxA and NoxB along the developmental cycle, except for a transient 5-fold increase in NoxA messenger at 2 h into development. The differences in expression might possibly reflect strain differences between JH10 (this work) and AX4 (in the database). The transcript of *noxC* was present in low amounts in vegetative cells, increasing progressively during aggregation to reach a maximal level of expression during the final stages of morphogenesis. *p22^{phox}* and *p67^{phox}* transcripts were found in vegetative cells and decreased rapidly after the vegetative stage.

To test possible cell-type specificity in the expression of the various NADPH oxidases, RT-PCR was performed on

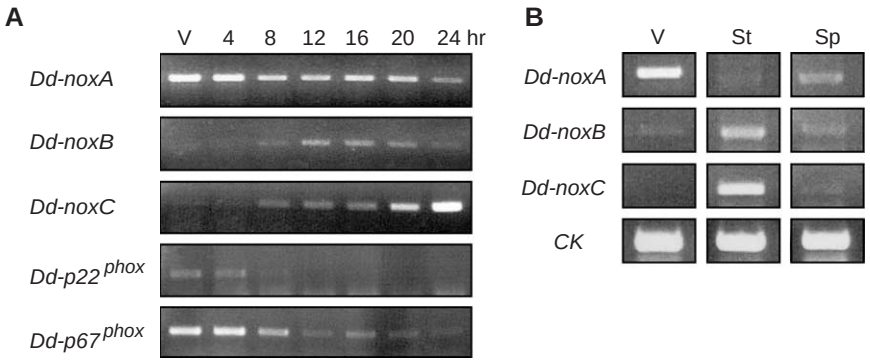

Fig. 4. Temporal and cell-type specific expression of the genes encoding the NADPH oxidase components in *D. discoideum*. (A) cDNA was synthesised by reverse transcriptase, starting from total RNA from vegetative amoebae or cells filter-developed on non nutritive Na/K Pi-buffered agar plates for 4, 8, 12, 16 and 24 h. Genes of interest were then amplified in a second step of the RT-PCR with a couple of specific primers. (B) RT-PCR reaction on total RNA from vegetative amoebae (V), stalk cells (St) or spore cells (Sp). The constitutively expressed casein kinase gene (*CK*) was used as control for equal loading.

RNA purified from stalk and spore subpopulations. *noxA* was expressed mostly in spores, *noxB* and *noxC* mostly in stalk cells (Fig. 4B).

3.4. Superoxide production by Dictyostelium Nox isoforms

The production of superoxide by intact vegetative *Dictyostelium* amoebae was measured by the standard ferricytochrome *c* assay. Compared with neutrophil and phagocyte NADPH oxidase (Nox2), no significant superoxide generation could be detected. Attempts to develop a cell-free reconstituted system using isolated membranes plus cytosol together with anionic amphiphiles such as arachidonic acid or lithium dodecylsulfate gave inconclusive results in view of the high reductase activity associated with *Dictyostelium* cytosol, a feature reminiscent of the phenomenon described in mammalian systems [57]. To obviate this handicap, heterologous activity measurements were performed with human cytosol and *Dictyostelium* membranes. The reconstituted oxidase activity was low and approximately less than 5% of that measured with the neutrophil system (data not shown). With intact cells, NBT assays on the parental and *nox*-null mutant strains (see below) were not statistically different. XTT assays showed reduced activities in *noxB*- and *noxA/noxB*-null strains, but the other mutants had activities similar to parent type JH10, as shown in Table 2. More sensitive assays using either dihydroethidine or luminol showed no evidence of NADPH oxidase activity.

Measurement of the superoxide production was also performed in developed cells [58]. For this, cells were pulsed for 4 h with low concentrations of cAMP (30 nM), followed by the addition for 1 h of 1 mM cAMP. Assaying protein samples from cells treated this way did not reveal any modulation of their NADPH oxidase activity (not shown).

3.5. NADPH oxidase null strains multiply normally

To investigate the physiological function of NADPH oxidases in *D. discoideum*, the three Nox genes and the $p22^{phox}$ gene were individually invalidated by homologous recombination in JH10 cells to obtain the single *noxA*, *-B*, *-C* or $p22^{phox}$ null strains. The double knockout of the 2 isoforms expressed in vegetative conditions, $noxA^-/noxB^-$, did not alter the viability of the mutants obtained, an indication that the genes being considered are not essential genes. Growth of the mutants by macropinocytosis of axenic medium or by phagocytosis of *K. aerogenes* lawns was identical to that for parental JH10 (data not shown).

3.6. NADPH oxidase mutants are arrested in their developmental program

The single disruptants $noxA^-$, $noxB^-$ and $noxC^-$ and $p22^-$ were plated on non-nutritive agar plates to follow their multicellular development. The aggregation of individual cells proceeded at a rate comparable to that of parent type cells. Past the aggregation stage, the mounds formed single or multiple finger-like protrusions and failed to generate wild-type-looking fruiting bodies. No spores were ever produced (Fig. 5B, D–G). Interestingly, the same block, in terms of timing and final phenotype, was observed for $noxA^-$, $noxB^-$, $noxC^-$, and $p22^{phox}$-null strains and the $noxA^-/noxB^-$ double knockout strain. In the case of $noxA^-$

Table 2
XTT assay of superoxide generation

Strains and relevant genotypes	XTT reduction (pmol/min)
JH10 (parent type, thy^-)	24.4 ± 1.4
$noxA^-$ (thy^+)	18.8 ± 3.2
$noxA^-$ (thy^-, bs^r)	28.2 ± 1.4
$noxA^-noxB^-$ (thy^+, bs^r)	4.5 ± 2.3
$noxB^-$ (thy^-, bs^r)	9.7 ± 2.8
$noxC^-$ (thy^-, bs^r)	19.4 ± 3.7
$p22^{phox-}$ (thy^-, bs^r)	20.8

bs^r: resistance to the antibiotic blasticidin S. Tiron-sensitive XTT reduction was measured at a cell density of 2×10^7/ml [42]. The data are the means ± S.E. of three experiments, except for $p22^{phox-}$ (one experiment).

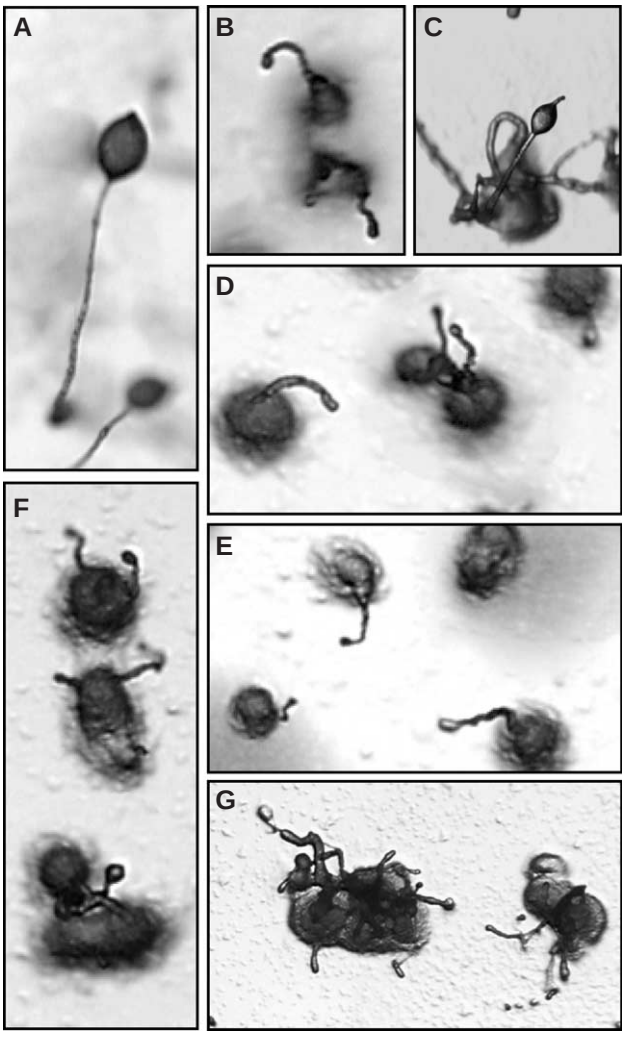

Fig. 5. Developmental morphology of *nox* and $p22^{phox}$ null strains. Development of the various knockout mutants was determined in non-nutritive Na/K–Pi buffered agar plates. Photographs (×24) were taken on a Nikon SMZ-U dissecting microscope equipped with a Sony 3CCD camera after 30 h of development. (A) Parent, (B) $noxA^-$, (C) $noxA^-$ overexpressing $NoxA_{myc2}$, (D) $noxB^-$, (E) $noxC^-$, (F) $p22^{phox-}$ and (G) $noxA^-/noxB^-$.

mutant, the overexpression of $NoxA_{myc2}$, under the control of the *act15* promoter, lead to the final differentiation of fruiting bodies containing viable spores able to germinate (Fig. 5C).

To assess the impact of the $noxA^-/noxB^-$ knockout on cell type differentiation, we examined the expression of the reporter *lacZ* gene under the control of the prestalk-specific promoter *ecmA*, the prespore-specific promoter *SP60* and the spore-specific promoter *SpiA*. The $noxA^-/noxB^-$ mutant carrying the constructs *SP60/lacZ*, *SpiA/lacZ* and *ecmA/lacZ*, stained with X-Gal, showed only expression of prestalk genes (Fig. 6A–D). These results demonstrate an early block in the differentiation pathway, with a major effect on prespore gene expression and a lesser effect on stalk differentiation.

3.7. The developmental defect of NADPH oxidase component-null strains is cell autonomous and not rescued by exogenous H_2O_2

The products of the NADPH oxidase activities are the highly diffusible but short-lived ROS, eventually yielding H_2O_2. To test whether these reaction products were necessary second messengers in the *Dictyostelium* developmental program, we performed chimera experiments. $noxA^-/noxB^-$ cells carrying the *act15/lacZ* reporter construct were mixed with parental cells and tested for their ability to participate in development. In the mound (Fig. 6E), $noxA^-/noxB^-$ cells essentially distributed as clusters at the prestalk–prespore boundary. Null cells stayed at the

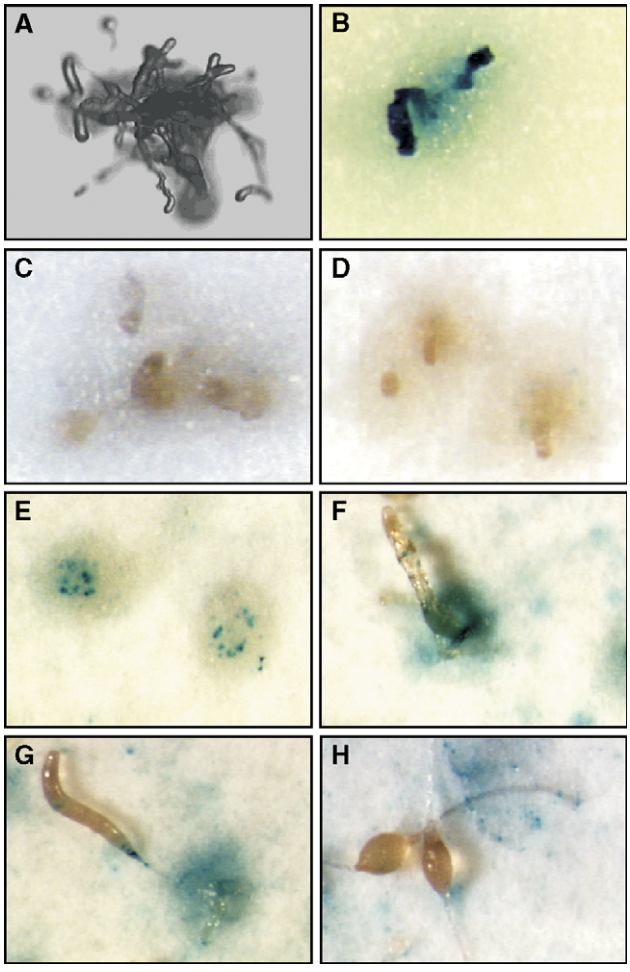

Fig. 6. Expression of developmental-specific-genes and chimeric organism analysis of $noxA^-/noxB^-$ strain. The $noxA^-/noxB^-$ double knockout (A) was transformed with the reporter gene *lacZ* under the control of the prestalk-specific promoter *ecmA* (B), the prespore-specific promoter *SP60* (C) and the spore-specific promoter *SpiA* (D). The final structures (B–D) were stained as described in Materials and methods. Double knockout $noxA^-/noxB^-$ cells carrying the reporter constructs *act15/lacZ* were allowed to coaggregate in a 1:3 ration with parental cells to form chimeric organisms. Aggregates were stained at different developmental stages corresponding to mound (E), culmination (F, G) and fruiting body (H). Photographs were taken on a Nikon SMZ-U dissecting microscope equipped with a Sony 3CCD colour video camera.

basis of the second finger (Fig. 6F–G) and were excluded from the mature fruiting body, leaving patches of blue stained cells on the substratum (Fig. 6H).

With the same areas of investigation in mind, we tested the effect of adding H_2O_2 to the developing null strains. The addition of increasing concentrations of H_2O_2 to the agar layer on which *noxA*$^-$ cells were spread did not rescue development, but H_2O_2 at a concentration of 6 mM inhibited aggregation (data not shown). These results strongly suggest that the altered development of the mutant cells is not due to the absence of a diffusible morphogen such as H_2O_2.

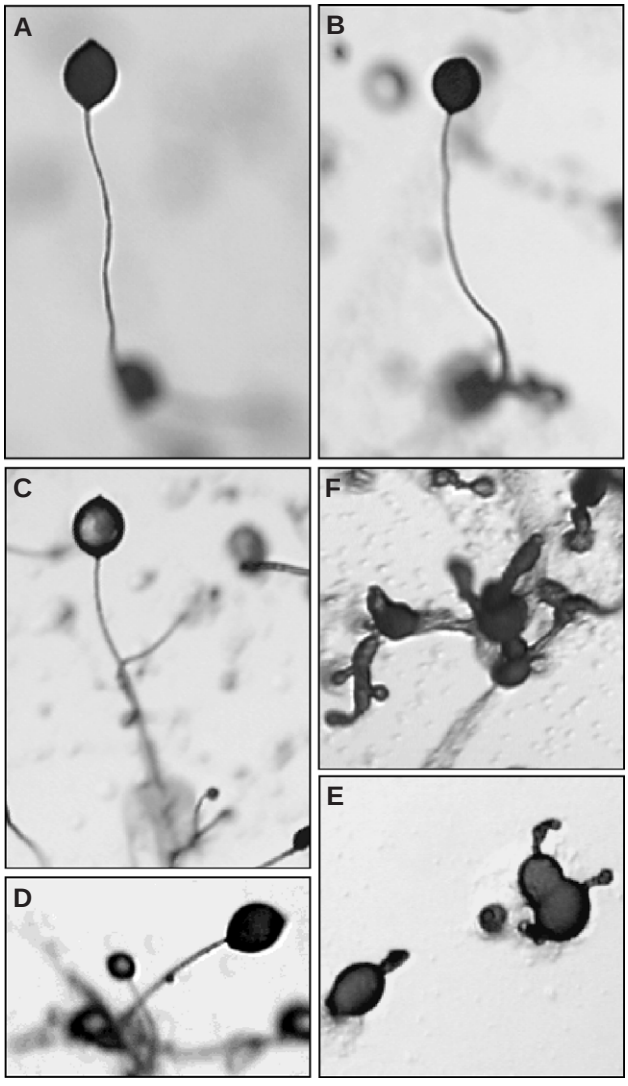

Fig. 7. Suppression of the *nox*$^-$ developmental phenotype by the *alg-2B* knockout. Null mutants of *noxA*, *noxB* and *noxC* were constructed using the JH10 *alg-2B* null strain as parent [36]. ALG-2B, under the control of the *act15* promoter, was overexpressed in the pEXP4$^+$ vector in the double knockout strain *noxA*$^-$/*alg-2B*$^-$. The various strains were developed on non-nutritive Na/K–Pi buffered agar plates and pictures were taken after 30 h of development (×24) on a Nikon SMZ-U dissecting microscope, equipped with a Sony 3CCD camera. (A) *alg-2B*$^-$, (B) *alg-2B*$^-$/*noxA*$^-$, (C) *alg-2B*$^-$/*noxB*$^-$, (D) *alg-2B*$^-$/*p22*$^{phox-}$, (E) *alg-2B*$^-$/*noxC*$^-$, and (F) *alg-2B*$^-$/*noxA*$^-$ overexpressing ALG-2B.

3.8. Disruption of alg-2B suppresses the developmental phenotype of noxA, noxB and p22^{phox} *knockouts*

The cross-talk between ROS and calcium signalling pathways observed in plants [24] prompted us to test the effect of the ablation of the penta EF-hand calciprotein, ALG-2B, [36,59] in *nox* and *p22*^{phox} null mutants. The ALG-2A/B proteins are non-essential and *alg-2A* and *alg-2B* null strains display a normal developmental phenotype [36]. In contrast to the developmentally arrested *noxA*$^-$, *noxB*$^-$ and *p22*$^{phox-}$ strains, the double knockout strains *alg-2B*$^-$/*noxA*$^-$ and *alg-2B*$^-$/*noxB*$^-$, as well as *alg-2B*$^-$/*p22*$^{phox-}$, showed a restored developmental phenotype (Fig. 7B–D). Furthermore, the overexpression of *alg-2B* in these double knockout strains led to the initial altered phenotype observed for *noxA*$^-$ (Fig. 7F) *noxB*$^-$ and *p22*$^{phox-}$(not shown). These results demonstrate that ALG-2B inactivation acts as a suppressor of *noxA*, *noxB* and *p22*^{phox} mutations. In contrast, the ablation of ALG-2B in the *noxC*$^-$ (Fig. 7E) strain did not rescue the developmental defect of the *noxC* null mutant.

4. Discussion

In this work, we report the cloning of three homologs of the large subunit of NADPH oxidase (NoxA, -B, -C), a homolog of the small subunit p22^{phox} and a homolog of the cytosolic factor p67^{phox}. The three *Dictyostelium nox* genes code for proteins from different subfamilies, one closely resembling human Nox2 and two with N-terminal extensions, among which one had two calcium-binding domains of the EF-hand type. The p22^{phox} homolog, although lacking the polyproline region found in the human protein and implicated in p47^{phox} binding, exhibits a strong sequence homology and shares the secondary structure of the human p22^{phox}. A possible function would be to stabilise the gp91^{phox} subunit as previously suggested [6]. *Dictyostelium* p67^{phox} is longer than human p67^{phox} or NOXA1, but the overall domain structure of the protein is conserved. One main difference between mammalian and *Dictyostelium* p67^{phox} is the absence of the activation domain (L199-D212) required for phagocyte oxidase activation [60], but recently a p67^{phox} without functional activating domain was shown to remain effective in activating the human isoform Nox3 [61]. These five proteins, NoxA, -B, -C, p22^{phox} and p67^{phox}, may constitute minimal catalytic complexes in *D. discoideum*.

Up to now, we have no evidence to show whether the p22^{phox} and p67^{phox} subunits interact with all three Nox isoforms in *D. discoideum*. No homolog for p47^{phox} or NOXO1 could be found, and the absence of this cytosolic factor in *D. discoideum* is accompanied by the absence of its binding domains on the large and small NADPH oxidase subunits and on p67^{phox}. However, the absence of two out of three p47^{phox} binding sequences on a Nox isoform may not

be a sufficient indication for the absence of interactions with that cytosolic factor. Indeed, in human Nox1 that lacks the same $p47^{phox}$ binding sequences as *Dictyostelium* Nox proteins is still able to interact with the $p47^{phox}$ homolog NOXO1 [49]. The third cytosolic factor $p40^{phox}$ is also missing. The small G protein Rac plays a capital regulatory role in the activation of neutrophil Nox2 [11,62]. *Dictyostelium* possesses six members of the Rac GTPase subfamily [52,53,63], with Rac1A, -B and -C showing the greatest homology with Rac2 in neutrophils. All of the Rac residues that are involved in the interface with $p67^{phox}$ are conserved, suggesting that the same activation process might occur in *D. discoideum*.

The presence of three NADPH oxidase isoforms in a simple eukaryote such as *D. discoideum* might appear striking. Several reasons for the multiplicity of isoforms may be proposed. First, the isoforms belong to two subfamilies, the activity of which is differently regulated, with NoxA and NoxB resembling Nox2/Nox4 homologs and NoxC resembling the calcium-activated Nox5 homolog. Second, their patterns of expression vary temporally and spatially during differentiation, with NoxA being expressed throughout the developmental cycle, and preferentially in spores, NoxB and -C being expressed late, and preferentially in stalk cells. The expression pattern of $p22^{phox}$ and $p67^{phox}$ early during the developmental cycle might provide an additional level of complexity, depending on which Nox isoform they interact with.

In order to obtain insight into the function of NADPH oxidases in *D. discoideum*, we have used homologous recombination to generate null mutants in the genes coding for the three Nox proteins and the small $p22^{phox}$ subunit. The fact that such mutants could be obtained indicates that the genes coding for the components of the NADPH oxidases are not essential genes. *Dictyostelium* Nox activity measurements, performed on parental and null strains, gave no significant results, with tests based on cytochrome *c* or NBT reduction on whole cells and reconstituted complexes, indicating that amoebal NADPH oxidases do not follow the paradigm established for neutrophil Nox2, but resemble the oxidase of Epstein Barr virus immortalised B lymphocytes [64], and human Nox homologs that exhibit modest superoxide-generating activities. Perhaps a too high level of superoxide generation would lead to cytotoxic effects. Assays based on luminol or dihydroethidine were negative, confirming the reported absence of luminol-enhanced chemiluminescence in *Dictyostelium* [65]. The generation of superoxides by *D. discoideum* cells is disclosed by the reduction of XTT, as described in a recent work [42]. The activity generating superoxide is very low and the origin of superoxide anions to NADPH oxidases is only partially validated through the use of Nox mutants, pointing to a specific role for NoxB (Table 2). The absence of a NoxC-associated NADPH oxidase activity in vegetative cells is not surprising, as *noxC* is expressed only late in development. The absence of a clearly attributable NoxA activity, when the disruption of its gene generates a developmental phenotype, might suggest that NoxA is activated during development by a still unknown mechanism. Conditioned *D. discoideum* growth medium contains a heat-labile factor that stimulates superoxide production [42]. Whether and how Nox activities are regulated by this factor remains to be established.

The vegetative functions of *nox*-null mutants and, in particular, axenic growth did not display any remarkable defect. The bacterial phagocytic capacity of *D. discoideum* is a potential mechanism in which the Nox proteins might be implicated. It is noticeable that whatever the missing component of the NADPH oxidases (NoxA, -B, -C, and $p22^{phox}$), the growth of *D. discoideum* on bacterial lawns was unaffected. Feeding on live bacteria represents an integrated mechanism dependent on prey capture, killing and digestion. Our data indicate that none of these parameters, together with *D. discoideum* proliferation, is regulated in any detectable way by the functioning of Nox enzymes.

Starvation of *D. discoideum* amoebae induces a developmental program that leads to the formation of a multicellular structure comprising dead stalk cells supporting a mass of dormant spores awaiting for optimal conditions to germinate. Peroxide and superoxide species are produced during the early stages of *Dictyostelium* development and superoxide has been involved in development [42,65]. Indeed, major defects in development and morphogenesis are observed in *D. discoideum* null strains for components of NADPH oxidase isoforms, defects that compromise the formation of mature fruiting bodies. A striking observation is that the developmental phenotypes of all of our null-mutants ($noxA^-$, $noxB^-$, $noxC^-$, $noxA^-/noxB^-$, and $p22^{phox-}$) are very similar, with tiny fingers extending from a mound-shaped aggregate. Although this phenotypic similarity might suggest a block in a single pathway, the suppression effect of the calciprotein ALG-2B (see below) on some *nox*-null strains ($noxA^-$ and $noxB^-$) and not others ($noxC^-$) indicates that this is not the case. The function of Nox proteins restricted to the multicellular phase of *D. discoideum* life supports the recently proposed idea that NADPH oxidases are indeed enzymes specifically involved in intercellular signalling processes [28], and we show here that the superoxide-producing NADPH oxidases participate in the signalling for proper differentiation. Interference of ROS production and development has previously been inferred through the overexpression of the scavenging enzyme superoxide dismutase, which produces aggregation-deficient cells when plated at low cell density [42]. The defect revealed by the disruption of *D. discoideum* Nox isoforms is subsequent to the aggregation phase. These two sets of results point to several sites in development where ROS could be implicated.

The proportioning of cell types is strongly affected in the *noxA* knockout, expression of prestalk-specific *ecmA* gene being correlated with the absence of the expression of

prespore- and spore-specific genes. The application of a hydroxamic acid derivative as an inhibitor of the mitochondrial alternative oxidase induces the formation of cell aggregates comprising dead stalk cells; this result has been taken as an argument in favour of the scavenging mitochondrial ROS from an alternative respiratory chain functions [66] and the involvement of ROS in the program leading to the death of stalk cells [67]. These observations might suggest that ROS are able to deliver different signals leading to the expression of either pre-spore or pre-stalk genes and later in development, to the death of stalk cells.

Mixing parental and mutant cells or adding H_2O_2 to the developing mutant cells does not rescue a normal phenotype of development, so it is therefore impossible to pinpoint the nature of the mediator (superoxide, H_2O_2) used in the cell-fate signalling process. At high concentration, H_2O_2 inhibited cell aggregation, but the effect was most probably due to the rapid killing of cells by this high concentration of H_2O_2 [68].

As with *A. thaliana* [24] and *Aspergillus nidulans* [69], *D. discoideum* represents an additional species in which NADPH oxidases control development. In plants, all NADPH oxidase isoforms contain EF-hands, indicating a direct regulatory function of Ca^{2+} on these enzymes, possibly through the direct activation mechanism proposed recently for Nox5 [16]. Furthermore, ROS regulate plant growth by activating Ca^{2+}-channels [24]. The likelihood of there being a role for intracellular calcium in the regulation of *D. discoideum* development has been demonstrated in experiments showing that overexpression of the plasma membrane calcium pump induces an arrest in development, with the formation of aberrant finger-like structures [70]. Interestingly, the developmental phenotype is similar to the phenotypes observed here for the *nox*-null mutants, supporting the hypothesis of an interplay between ROS and Ca^{2+}-signalling pathways. Among the three *D. discoideum* Nox isoforms, only NoxC harbours 2 EF-hands, while a knockout of any of the three isoforms leads to the same arrest of the developmental cycle. This means that Ca^{2+} cannot directly regulate the activity of all three *Dictyostelium* Nox proteins. Nevertheless, its intracellular concentration might be controlled by the availability of these Nox isoforms, possibly through an action on Ca^{2+}-channels (for review, [71]).

The cross-talk between ROS and Ca^{2+} signalling pathways is further illustrated in a suppressor experiment, where the ablation of the penta EF-hand calciprotein ALG-2B rescues the development of *noxA*-, *noxB*- and $p22^{phox}$-null strain, but not of *noxC*-null strain. This could mean that ALG-2B acts as an inhibitor of a downstream effector of the Nox signalling pathway, and that the physiological functioning of NoxA- and -B leads to the relief of this inhibition, possibly by inducing a Ca^{2+}-dependent heterodimerisation with ALG-2A, subsequent to an increase in the concentration of this ion [36]. In the absence of the two Nox proteins, the removal of ALG-2B could then lift the inhibitory block and, as a consequence, development could proceed normally. Signalling by NoxC that possesses its own calcium-binding EF-hands does not converge with the ALG-2B calciprotein pathway. We are currently undertaking a more detailed exploration of how ROS production and calcium signalling pathways are interlaced.

Acknowledgements

This work was supported by research funds from the Commissariat à l'Energie Atomique, the Centre National de la Recherche Scientifique (UMR5092) and the Faculté de Médecine, Université Joseph Fourier (Grenoble, France). B. Lardy was supported by the Ministère de l'Education Nationale Recherche et Technologie and by the Association de Recherche contre le Cancer. The sequencing and the analysis of the genome of *D. discoideum* is an international collaboration between the University of Cologne, Germany (Cologne), the Institute of Molecular Biotechnology in Jena, Germany (Jena), the Baylor College of Medicine in Houston, USA (Baylor), Medical Research Council Laboratory of Molecular Biology (LMB), University of Dundee, the Pasteur Institute in Paris, France (Pasteur), and the Sanger Centre in Hinxton, England (Sanger). The gene expression data have been posted thanks to the Baylor Functional Genomics team lead by Gad Shaulsky, John Halter and Adam Kuspa, and Negin Iranfar, Danny Fuller, and William Loomis at UCSD. We thank Nelly Bennett, François Boulay, Pierre Cosson, Marie-Claire Dagher, Jacques Doussière and Pierre Vignais for helpful discussions.

References

[1] D.B. Drath, M.L. Karnovsky, Superoxide production by phagocytic leukocytes, J. Exp. Med. 141 (1975) 257–262.
[2] P.G. Heyworth, A.R. Cross, J.T. Curnutte, Chronic granulomatous disease, Curr. Opin. Immunol. 15 (2003) 578–584.
[3] L. Yu, M.T. Quinn, A.R. Cross, M.C. Dinauer, Gp91(phox) is the heme binding subunit of the superoxide-generating NADPH oxidase, Proc. Natl. Acad. Sci. U. S. A. 95 (1998) 7993–7998.
[4] G.M. Bokoch, U.G. Knaus, NADPH oxidases: not just for leukocytes anymore!, Trends Biochem. Sci. 28 (2003) 502–508.
[5] J.D. Lambeth, G. Cheng, R.S. Arnold, W.A. Edens, Novel homologs of gp91phox, Trends Biochem. Sci. 25 (2000) 459–461.
[6] P.V. Vignais, The superoxide-generating NADPH oxidase: structural aspects and activation mechanism, Cell. Mol. Life Sci. 59 (2002) 1428–1459.
[7] A.P. Bouin, N. Grandvaux, P.V. Vignais, A. Fuchs, p40(phox) is phosphorylated on threonine 154 and serine 315 during activation of the phagocyte NADPH oxidase. Implication of a protein kinase c-type kinase in the phosphorylation process, J. Biol. Chem. 273 (1998) 30097–30103.
[8] F. Kuribayashi, H. Nunoi, K. Wakamatsu, S. Tsunawaki, K. Sato, T. Ito, H. Sumimoto, The adaptor protein p40(phox) as a positive regulator of the superoxide-producing phagocyte oxidase, EMBO J. 21 (2002) 6312–6320.
[9] S. Berthier, M.H. Paclet, S. Lerouge, F. Roux, S. Vergnaud, A.W. Coleman, F. Morel, Changing the conformation state of cytochrome

*b*558 initiates NADPH oxidase activation: MRP8/MRP14 regulation, J. Biol. Chem. 278 (2003) 25499–25508.
[10] J. Doussiere, F. Bouzidi, P.V. Vignais, The S100A8/A9 protein as a partner for the cytosolic factors of NADPH oxidase activation in neutrophils, Eur. J. Biochem. 269 (2002) 3246–3255.
[11] A. Abo, A. Boyhan, I. West, A.J. Thrasher, A.W. Segal, Reconstitution of neutrophil NADPH oxidase activity in the cell-free system by four components: p67-phox, p47-phox, p21rac1, and cytochrome *b*-245, J. Biol. Chem. 267 (1992) 16767–16770.
[12] J.D. Lambeth, Nox/Duox family of nicotinamide adenine dinucleotide (phosphate) oxidases, Curr. Opin. Hematol. 9 (2002) 11–17.
[13] B. Lassegue, R.E. Clempus, Vascular NAD(P)H oxidases: specific features, expression, and regulation, Am. J. Physiol., Regul. Integr. Comp. Physiol. 285 (2003) R277–R297.
[14] J.D. Lambeth, NOX enzymes and the biology of reactive oxygen, Nat. Rev., Immunol. 4 (2004) 181–189.
[15] M. Geiszt, T.L. Leto, The Nox family of NAD(P)H oxidases: host defense and beyond, J. Biol. Chem. 279 (2004) 51715–51718.
[16] B. Banfi, F. Tirone, I. Durussel, J. Knisz, P. Moskwa, G.Z. Molnar, K.H. Krause, J.A. Cox, Mechanism of Ca^{2+} activation of the NADPH oxidase 5 (NOX5), J. Biol. Chem. 279 (2004) 18583–18591.
[17] X. De Deken, D. Wang, M.C. Many, S. Costagliola, F. Libert, G. Vassart, J.E. Dumont, F. Miot, Cloning of two human thyroid cDNAs encoding new members of the NADPH oxidase family, J. Biol. Chem. 275 (2000) 23227–23233.
[18] B. Caillou, C. Dupuy, L. Lacroix, M. Nocera, M. Talbot, R. Ohayon, D. Deme, J.M. Bidart, M. Schlumberger, A. Virion, Expression of reduced nicotinamide adenine dinucleotide phosphate oxidase (ThoX, LNOX, Duox) genes and proteins in human thyroid tissues, J. Clin. Endocrinol. Metab. 86 (2001) 3351–3358.
[19] B. Banfi, G. Molnar, A. Maturana, K. Steger, B. Hegedus, N. Demaurex, K.H. Krause, A Ca^{2+}-activated NADPH oxidase in testis, spleen, and lymph nodes, J. Biol. Chem. 276 (2001) 37594–37601.
[20] M. Geiszt, J. Witta, J. Baffi, K. Lekstrom, T.L. Leto, Dual oxidases represent novel hydrogen peroxide sources supporting mucosal surface host defense, FASEB J. 17 (2003) 1502–1504.
[21] R. Takeya, N. Ueno, K. Kami, M. Taura, M. Kohjima, T. Izaki, H. Nunoi, H. Sumimoto, Novel human homologues of p47phox and p67phox participate in activation of superoxide-producing NADPH oxidases, J. Biol. Chem. 278 (2003) 25234–25246.
[22] R.S. Arnold, J. Shi, E. Murad, A.M. Whalen, C.Q. Sun, R. Polavarapu, S. Parthasarathy, J.A. Petros, J.D. Lambeth, Hydrogen peroxide mediates the cell growth and transformation caused by the mitogenic oxidase Nox1, Proc. Natl. Acad. Sci. U. S. A. 98 (2001) 5550–5555.
[23] Y.A. Suh, R.S. Arnold, B. Lassegue, J. Shi, X. Xu, D. Sorescu, A.B. Chung, K.K. Griendling, J.D. Lambeth, Cell transformation by the superoxide-generating oxidase Mox1, Nature 401 (1999) 79–82.
[24] J. Foreman, V. Demidchik, J.H. Bothwell, P. Mylona, H. Miedema, M.A. Torres, P. Linstead, S. Costa, C. Brownlee, J.D. Jones, J.M. Davies, L. Dolan, Reactive oxygen species produced by NADPH oxidase regulate plant cell growth, Nature 422 (2003) 442–446.
[25] M.A. Torres, J.L. Dangl, J.D. Jones, *Arabidopsis* gp91phox homologues *AtrbohD* and *AtrbohF* are required for accumulation of reactive oxygen intermediates in the plant defense response, Proc. Natl. Acad. Sci. U. S. A. 99 (2002) 517–522.
[26] M.A. Torres, H. Onouchi, S. Hamada, C. Machida, K.E. Hammond-Kosack, J.D. Jones, Six *Arabidopsis thaliana* homologues of the human respiratory burst oxidase (gp91phox), Plant J. 14 (1998) 365–370.
[27] M. Sagi, R. Fluhr, Superoxide production by plant homologues of the gp91(phox) NADPH oxidase. Modulation of activity by calcium and by tobacco mosaic virus infection, Plant Physiol. 126 (2001) 1281–1290.
[28] H. Lalucque, P. Silar, NADPH oxidase: an enzyme for multicellularity? Trends Microbiol. 11 (2003) 9–12.
[29] W.F. Loomis, *Dictyostelium discoideum*. A Developmental System, Academic Press, New York, 1975.
[30] P.N. Devreotes, S.H. Zigmond, Chemotaxis in eukaryotic cells: a focus on leukocytes and *Dictyostelium*, Annu. Rev. Cell Biol. 4 (1988) 649–686.
[31] K.P. Janssen, M. Schleicher, *Dictyostelium discoideum*: a genetic model system for the study of professional phagocytes. Profilin, phosphoinositides and the *lmp* gene family in *Dictyostelium*, Biochim. Biophys. Acta 1525 (2001) 228–233.
[32] S. van Es, P.N. Devreotes, Molecular basis of localized responses during chemotaxis in amoebae and leukocytes, Cell. Mol. Life Sci. 55 (1999) 1341–1351.
[33] L. Kreppel, P. Fey, P. Gaudet, E. Just, W.A. Kibbe, R.L. Chisholm, A.R. Kimmel, dictyBase: a new *Dictyostelium discoideum* genome database, Nucleic Acids Res. 32 (2004) D332–D333.
[34] K. Sutoh, A transformation vector for *Dictyostelium discoideum* with a new selectable marker bsr, Plasmid 30 (1993) 150–154.
[35] J.L. Dynes, R.A. Firtel, Molecular complementation of a genetic marker in *Dictyostelium* using a genomic DNA library, Proc. Natl. Acad. Sci. U. S. A. 86 (1989) 7966–7970.
[36] L. Aubry, S. Mattei, B. Blot, R. Sadoul, M. Satre, G. Klein, Biochemical characterization of two analogues of the apoptosis-linked gene 2 protein in *Dictyostelium discoideum* and interaction with a physiological partner in mammals, murine Alix, J. Biol. Chem. 277 (2002) 21947–21954.
[37] W. Nellen, S. Datta, C. Reymond, A. Sivertsen, S. Mann, T. Crowley, R.A. Firtel, Molecular biology in *Dictyostelium*: tools and applications, Methods Cell Biol. 28 (1987) 67–100.
[38] L. Haberstroh, R.A. Firtel, A spatial gradient of expression of a cAMP-regulated prespore cell-type-specific gene in *Dictyostelium*, Genes Dev. 4 (1990) 596–612.
[39] S.K.O. Mann, P.N. Devreotes, S. Eliott, K. Jermyn, A. Kuspa, M. Fechheimer, R. Furukawa, C.A. Parent, J. Segall, G. Shaulsky, P.H. Vardy, J. Williams, K.L. Williams, R.A. Firtel, in: J.E. Celis (Ed.), Cell Biology—A Laboratory Handbook, Ac. Press, San Diego, CA, 1994, pp. 412–451.
[40] Y. Bromberg, E. Pick, Unsaturated fatty acids stimulate NADPH-dependent superoxide production by cell-free system derived from macrophages, Cell. Immunol. 88 (1984) 213–221.
[41] R.A. Heyneman, R.E. Vercauteren, Activation of a NADPH oxidase from horse polymorphonuclear leukocytes in a cell-free system, J. Leukoc. Biol. 36 (1984) 751–759.
[42] G. Bloomfield, C. Pears, Superoxide signalling required for multicellular development of *Dictyostelium*, J. Cell Sci. 116 (2003) 3387–3397.
[43] J.D. Thompson, D.G. Higgins, T.J. Gibson, CLUSTAL W: improving the sensitivity of progressive multiple sequence alignment through sequence weighting, position-specific gap penalties and weight matrix choice, Nucleic Acids Res. 22 (1994) 4673–4680.
[44] D. Roos, M. de Boer, F. Kuribayashi, C. Meischl, R.S. Weening, A.W. Segal, A. Ahlin, K. Nemet, J.P. Hossle, E. Bernatowska-Matuszkiewicz, H. Middleton-Price, Mutations in the X-linked and autosomal recessive forms of chronic granulomatous disease, Blood 87 (1996) 1663–1681.
[45] F.R. DeLeo, L. Yu, J.B. Burritt, L.R. Loetterle, C.W. Bond, A.J. Jesaitis, M.T. Quinn, Mapping sites of interaction of p47-phox and flavocytochrome *b* with random-sequence peptide phage display libraries, Proc. Natl. Acad. Sci. U. S. A. 92 (1995) 7110–7114.
[46] I. Dahan, I. Issaeva, Y. Gorzalczany, N. Sigal, M. Hirshberg, E. Pick, Mapping of functional domains in the p22(phox) subunit of flavocytochrome *b*(559) participating in the assembly of the NADPH oxidase complex by "peptide walking", J. Biol. Chem. 277 (2002) 8421–8432.
[47] Y. Groemping, K. Lapouge, S.J. Smerdon, K. Rittinger, Molecular basis of phosphorylation-induced activation of the NADPH oxidase, Cell 113 (2003) 343–355.

[48] M.J. Macias, S. Wiesner, M. Sudol, WW and SH3 domains, two different scaffolds to recognize proline-rich ligands, FEBS Lett. 513 (2002) 30–37.
[49] B. Banfi, R.A. Clark, K. Steger, K.H. Krause, Two novel proteins activate superoxide generation by the NADPH oxidase NOX1, J. Biol. Chem. 278 (2003) 3510–3513.
[50] S. Grizot, F. Fieschi, M.C. Dagher, E. Pebay-Peyroula, The active N-terminal region of p67phox. Structure at 1.8 A resolution and biochemical characterizations of the A128V mutant implicated in chronic granulomatous disease, J. Biol. Chem. 276 (2001) 21627–21631.
[51] K. Lapouge, S.J. Smith, P.A. Walker, S.J. Gamblin, S.J. Smerdon, K. Rittinger, Structure of the TPR domain of p67phox in complex with Rac.GTP, Mol. Cell 6 (2000) 899–907.
[52] J. Bush, K. Franek, J. Cardelli, Cloning and characterization of seven novel *Dictyostelium discoideum* rac-related genes belonging to the rho family of GTPases, Gene 136 (1993) 61–68.
[53] M. Dumontier, P. Hocht, U. Mintert, J. Faix, Rac1 GTPases control filopodia formation, cell motility, endocytosis, cytokinesis and development in *Dictyostelium*, J. Cell Sci. 113 (2000) 2253–2265.
[54] U. Kikkawa, S.K. Mann, R.A. Firtel, T. Hunter, Molecular cloning of casein kinase II alpha subunit from *Dictyostelium discoideum* and its expression in the life cycle, Mol. Cell. Biol. 12 (1992) 5711–5723.
[55] N. Iranfar, D. Fuller, W.F. Loomis, Genome-wide expression analyses of gene regulation during early development of *Dictyostelium discoideum*, Eukaryot. Cell 2 (2003) 664–670.
[56] N. Van Driessche, C. Shaw, M. Katoh, T. Morio, R. Sucgang, M. Ibarra, H. Kuwayama, T. Saito, H. Urushihara, M. Maeda, I. Takeuchi, H. Ochiai, W. Eaton, J. Tollett, J. Halter, A. Kuspa, Y. Tanaka, G. Shaulsky, A transcriptional profile of multicellular development in *Dictyostelium discoideum*, Development 129 (2002) 1543–1552.
[57] H. Zhu, H. Qiu, H.W. Yoon, S. Huang, H.F. Bunn, Identification of a cytochrome *b*-type NAD(P)H oxidoreductase ubiquitously expressed in human cells, Proc. Natl. Acad. Sci. U. S. A. 96 (1999) 14742–14747.
[58] S.K. Mann, R.A. Firtel, Two-phase regulatory pathway controls cAMP receptor-mediated expression of early genes in *Dictyostelium*, Proc. Natl. Acad. Sci. U. S. A. 86 (1989) 1924–1928.
[59] S. Ohkouchi, K. Nishio, M. Maeda, K. Hitomi, H. Adachi, M. Maki, Identification and characterization of two penta-EF-hand Ca(2+)-binding proteins in *Dictyostelium discoideum*, J. Biochem. (Tokyo) 130 (2001) 207–215.
[60] C.H. Han, J.L. Freeman, T. Lee, S.A. Motalebi, J.D. Lambeth, Regulation of the neutrophil respiratory burst oxidase. Identification of an activation domain in p67(phox), J. Biol. Chem. 273 (1998) 16663–16668.
[61] G. Cheng, D. Ritsick, J.D. Lambeth, Nox3 regulation by NOXO1, p47phox, and p67phox, J. Biol. Chem. 279 (2004) 34250–34255.
[62] O. Dorseuil, A. Vazquez, P. Lang, J. Bertoglio, G. Gacon, G. Leca, Inhibition of superoxide production in B lymphocytes by rac antisense oligonucleotides, J. Biol. Chem. 267 (1992) 20540–20542.
[63] F. Rivero, H. Dislich, G. Glockner, A.A. Noegel, The *Dictyostelium discoideum* family of Rho-related proteins, Nucleic Acids Res. 29 (2001) 1068–1079.
[64] M.H. Paclet, A.W. Coleman, J. Burritt, F. Morel, NADPH oxidase of Epstein-Barr-virus immortalized B lymphocytes. Effect of cytochrome *b*(558) glycosylation, Eur. J. Biochem. 268 (2001) 5197–5208.
[65] P.R. Fisher, P. Karampetsos, Z. Wilczynska, L.T. Rosenberg, Oxidative metabolism and heat shock-enhanced chemiluminescence in *Dictyostelium discoideum*, J. Cell Sci. 99 (1991) 741–750.
[66] S.I. Matsuyama, Y. Maeda, Involvement of cyanide-resistant respiration in cell-type proportioning during *Dictyostelium* development, Dev. Biol. 172 (1995) 182–191.
[67] W. Jarmuszkiewicz, M. Behrendt, R. Navet, F.E. Sluse, Uncoupling protein and alternative oxidase of *Dictyostelium discoideum*: occurrence, properties and protein expression during vegetative life and starvation-induced early development, FEBS Lett. 532 (2002) 459–464.
[68] M.X. Garcia, C. Foote, S. van Es, P.N. Devreotes, S. Alexander, H. Alexander, Differential developmental expression and cell type specificity of *Dictyostelium* catalases and their response to oxidative stress and UV-light, Biochim. Biophys. Acta 1492 (2000) 295–310.
[69] T. Lara-Ortiz, H. Riveros-Rosas, J. Aguirre, Reactive oxygen species generated by microbial NADPH oxidase NoxA regulate sexual development in *Aspergillus nidulans*, Mol. Microbiol. 50 (2003) 1241–1255.
[70] A.B. Cubitt, I. Reddy, S. Lee, J.G. McNally, R.A. Firtel, Coexpression of a constitutively active plasma membrane calcium pump with GFP identifies roles for intracellular calcium in controlling cell sorting during morphogenesis in *Dictyostelium*, Dev. Biol. 196 (1998) 77–94.
[71] J.I. Kourie, Interaction of reactive oxygen species with ion transport mechanisms, Am. J. Physiol. 275 (1998) C1–C24.